LBNL-39355
UC-404
Preprint

ERNEST ORLANDO LAWRENCE BERKELEY NATIONAL LABORATORY

Microstructure Refinement of Sintered Al_2O_3 by a Two-Step Sintering Technique

F.J.T. Lin, L.C. De Jonghe, and M.N. Rahaman
Materials Sciences Division

July 1996
Submitted for publication

REFERENCE COPY
Does Not
Circulate
Bldg. 50 Library.
LBNL-39355
Copy 1

DISCLAIMER

This document was prepared as an account of work sponsored by the United States Government. While this document is believed to contain correct information, neither the United States Government nor any agency thereof, nor the Regents of the University of California, nor any of their employees, makes any warranty, express or implied, or assumes any legal responsibility for the accuracy, completeness, or usefulness of any information, apparatus, product, or process disclosed, or represents that its use would not infringe privately owned rights. Reference herein to any specific commercial product, process, or service by its trade name, trademark, manufacturer, or otherwise, does not necessarily constitute or imply its endorsement, recommendation, or favoring by the United States Government or any agency thereof, or the Regents of the University of California. The views and opinions of authors expressed herein do not necessarily state or reflect those of the United States Government or any agency thereof or the Regents of the University of California.

LBNL-39355
UC-404

Microstructure Refinement of Sintered Al_2O_3 by a Two-Step Sintering Technique

Frank J.T. Lin and Lutgard C. De Jonghe

Department of Materials Science and Mineral Engineering
University of California
and
Materials Sciences Division
Ernest Orlando Lawrence Berkeley National Laboratory
University of California
Berkeley, California 94720

Mohamed N. Rahaman

Department of Ceramic Engineering
University of Missouri
Rolla, Missouri 65401

July 1996

This work was supported by the Director, Office of Energy Research, Office of Basic Energy Sciences, Materials Sciences Division, of the U.S. Department of Energy under Contract No. DE-AC03-76SF00098.

Microstructure Refinement of Sintered Al_2O_3 by a Two-Step Sintering Technique

Frank J. T. Lin* and Lutgard C. De Jonghe*
Materials Science Division, Lawrence Berkeley Laboratory, Berkeley, CA 94720, and
Department of Materials Science and Mineral Engineering, University of California,
Berkeley, CA 94720

Mohamed N. Rahaman*
Department of Ceramic Engineering, University of Missouri, Rolla, MO 65401

Abstract

For a few oxide ceramics, the use of an initial pre-coarsening step prior to densification (referred to as two-step sintering) has been observed to produce an improvement in the microstructural homogeneity during subsequent sintering. In the present work, the effect of a pre-coarsening step (50 h at 800 °C) on the subsequent densification and microstructural evolution of high quality Al_2O_3 powder compacts during constant heating rate sintering (4 °C/min to 1450 °C) was characterized in detail. The data were compared with those for similar compacts sintered conventionally (without the heat treatment step) and used to explore the mechanism of microstructural improvement during two-step sintering. After the pre-coarsening step, the average pore size was larger but the distribution in pore sizes was narrower than those for similar compacts sintered conventionally to 800 °C. In subsequent sintering, the microstructure of the pre-coarsened compact evolved in a more homogeneous manner and, at the same density, the amount of closed porosity was lower for the compacts sintered by the two-step technique compared to the conventional heating schedule. Furthermore, a measurably higher final density, a smaller average grain size and a narrower distribution in grain sizes were achieved with the two-step technique. The microstructural refinement produced by the two-step sintering technique is explained in terms of a reduction in the effects of differential densification and the resulting delay of the pore channel pinch-off to higher density.

*Member, the American Ceramic Society.

Supported by the Division of Materials Sciences, Office of Basic Energy Sciences, U.S. Department of Energy, under Contract No. DE-AC03-76SF00098.

I. Introduction

In general, the engineering properties of polycrystalline ceramics are controlled by the microstructure (e.g., density and grain size) of the fabricated material. However, microstructural defects or heterogeneities (e.g., large pores and abnormally large grains) in the fabricated material have a profound effect on those properties that are limited by mechanical failure. Failure events are almost always initiated at regions of physical or chemical heterogeneity. Density, grain size and the presence of microstructural heterogeneities must be carefully controlled to achieve improvements in the properties and reliability of ceramics.

Several fabrication routes are available for the production of ceramics with high density or a controlled grain size [1]. These include colloidal processing of powders with a controlled (narrow) distribution of sizes [2-4], pressure sintering, and the use of additives that are incorporated into solid solution [5-7] or form a discrete second phase, e.g., liquid phase sintering [7,8]. However, these fabrication routes can be uneconomical for many applications or can be difficult to apply successfully (e.g., choice of additives). Simple, economical routes to microstructural improvement are worthy of investigation.

Control of the heating schedule to manipulate the microstructure during sintering is an approach which has long been known to have the advantages of simplicity and economy. As discussed elsewhere [9], numerous efforts have been made to investigate its effectiveness. One of these is the "ratio controlled" approach in which the ratio of the densification rate to the coarsening rate is determined by the choice of temperature [1,10]. The merit of this approach has been demonstrated practically in the fast firing of Al_2O_3 [10,11], a system for which the conditions are favorable (i.e., the activation energy for densification is greater than that for grain growth) and for $BaTiO_3$ [12]. However, the fast firing technique has not been successful for MgO where the conditions are believed to be unfavorable [1]. Another method is "rate controlled sintering" in which attempts are made to keep the rate of densification approximately constant by controlling the temperature [13] and a related two-peak firing [14]. The two-peak method was

effective in the producion of sodium beta"-alumina, but in general the results of rate controlled sintering have been erratic and its merits remain unclear.

The ratio controlled approach is based primarily on a consideration of the kinetics of the densification and coarsening and may be more applicable to systems in which the microstructure is relatively homogeneous or develops in a relatively homogeneous manner. However, it has been well demonstrated that, in addition to scaling (particle size) effects, the homogeneity of the green microstructure can have a significant effect on the densification and grain growth processes during sintering [15-20]. Microstructural heterogeneities (such as large pores, large grains and non-uniform packing) present in the green compact cannot normally be removed during conventional sintering. Furthermore, they lead to differential densification which can enhance their detrimental effects, reduce densification rates and limit the final density [21,22].

For three oxide ceramic systems investigated so far, i.e., MgO [23,24], ZnO [9,25] and Al_2O_3 [9,26], it has been demonstrated that a two-step sintering technique, involving an initial pre-coarsening step (e.g., 25-100 hours) prior to densification, leads to an improvement in the microstructural homogeneity during subsequent sintering. In addition, the materials produced by the two-step sintering technique generally have a slightly higher density, a smaller average grain size and a narrower grain size distribution when compared with similar materials produced by conventional sintering (i.e., without the initial heat treatment step). For the systems investigated so far, two-step sintering provides a simple route for refining the microstructure, particularly for powder systems with heterogeneous packing and with a wide distribution of particle sizes.

While the refinement of the microstructure has been clearly demonstrated by microscopy and density measurements, a detailed investigation of the microstructural evolution during two-step sintering has not been performed. It has been suggested that during the first step, coarsening of the microstructure by surface diffusion, vapor transport, or some combination of these two mechanisms, produces a more uniform microstructure by an Ostwald ripening process. The evolution to a more homogeneous microstructure can be expected, at least qualitatively, from the

trend of the porous system to evolve towards a quasi-steady state structure. Such steady state structural distributions are generally significantly narrower than what is usually produced in a powder compact [9]. Enhanced neck formation in the pre-coarsened compact is also expected to produce a stronger system which is better able to resist differential densification, thereby limiting damage during subsequent sintering. The combination of a more uniform microstructure and the stronger compact produced by pre-coarsening is believed to be responsible for the microstructural refinement in subsequent sintering. Experimentally, Chu et al [9] found for ZnO that a pre-coarsening step for 90 h at 450 °C produced an increase in the particle size (1.7 times the starting particle size) and a modest reduction in the sintering stress (0.8 times that for the compact without the pre-coarsening treatment). However, the pore parameters were not characterized.

To explore the mechanism of microstructural refinement during the sintering stage of the two-step technique, Chu et al [9] used a semi-quantitative computational model to describe the evolution of the pore spacing during sintering. They found that compared to the conventionally sintered compact, the pore spacing for the pre-coarsened compact was larger in the earlier stage of sintering but smaller in the later stage of sintering. The smaller interpore spacing in the later stage of sintering was taken as a measure of microstructural uniformity. It was argued that the increased uniformity in the later stage of sintering allowed the pre-coarsened compact to stay in the open porosity state longer, leading to an inhibition of coarsening (grain growth). However, the evolution of the open and closed porosity during sintering was not investigated.

In the present work, a detailed investigation of the densification and microstructural evolution of Al_2O_3 during two-step sintering has been performed to explore the merits of the suggestions put forward for the microstructural refinement. Densification kinetics have been measured by dilatometry while microscopy, mercury porosimetry and gas adsorption have been used to characterize the spatial distribution of the grain and pore features, the average grain size

and grain size distribution, the porosity, average pore size and pore size distribution, and the surface area.

II. Experimental Procedure

(1) Powder Processing and Compaction

A commercial, high-purity a-Al_2O_3 powder (AKP-50; purity 99.995%; Sumitomo Chemical America, Inc., New York, NY) was used in the experiments. The as-received powder had an average particle size of 0.18 mm and a surface area of 10.4 m^2/g (as reported by the manufacturer). Prior to consolidation, the powder was processed to remove hard agglomerates. In the process, a dilute suspension (2 vol% solid) was prepared by dispersing the powder in deionized water (18.1 MW•cm) and adding nitric acid (HNO_3) to adjust the pH value in the range of 3 - 4. The suspension was agitated for 10 minutes with an ultrasonic probe (Model W-375, Heat System-Ultrasonics, Inc., Farmingdale, NY) and allowed to settle gravitationally for ~24 h, after which the supernatant was decanted (to separate it from the sedimented material) and dried rapidly under an infrared lamp while being stirred continuously.

The dried material was lightly ground with a mortar and pestle, passed through a 100 mesh (126 mm) nylon sieve and then ball-milled in the dry state using plastic milling media to produce a powder. The average particle size of the powder was measured by a centrifugal sedimentation technique based on the principle of liquid-phase photo-sedimentation (Model CAPA-700, Horiba Instruments Inc., Irvine, CA) at a rotational speed of 3000 rpm. The specific surface area was measured by nitrogen adsorption by the BET method (Digisorb 2600, Micromeritics Instrument Corp., Norcross, GA). Prior to the measurement, the powder was outgassed for 4 h at 400 °C in a vacuum.

Powder compacts for sintering were formed by uniaxial pressing in a WC-Co die followed by cold isostatic pressing under high pressure. No binder was used in the process. Die pressing was performed under a pressure of ~50 MPa to produce compacts (6.35 mm in diameter

by 6.2 mm) with a density of 0.53 of the theoretical density of α-Al_2O_3 (3.986 g/cm^3). After cold isostatic pressing under a pressure of ~1380 MPa, the relative density of the compacts increased to 0.60 ± 0.01.

(2) Sintering

Two sintering techniques were used in the experiments: two-step sintering and conventional sintering. Except for the prolonged isothermal heating used in the pre-coarsening stage of the two-step technique, conventional sintering was carried out under the same conditions used in the two-step technique. The sintering experiments were carried out in a dilatometer (Model 1600D; Edward Orton Jr. Ceramic Foundation, Westerville, OH) that allowed continuous monitoring of the shrinkage kinetics. A different green compact was used in each sintering run.

In preliminary experiments, it was found that the powder compacts started to show measurable densification at ~980 °C when heated at 4 °C/min. In the pre-coarsening stage of the two-step technique, a requirement is the achievement of significant coarsening without densification. Several combinations of temperature and time (800-1000 °C and 25-200 h) were investigated for the pre-coarsening stage and the microstructure produced by the heat treatment was observed by scanning electron microscopy of fracture surfaces. From these experiments, a heat treatment for 50 h at 800 °C was found to provide a reasonable balance between the duration of the experiment and achieving the microstructural requirement mentioned above.

In two-step sintering, the compact was heated at 10 °C/min to 800 °C, held at this temperature for 50 h and then heated at 4 °C/min to 1450 °C. The relative density, ρ, during sintering was determined from the initial relative density, ρ_o, and the measured shrinkage, $\Delta L/L_o$, using the equation:

$$\rho = \rho_o \left(1 - \frac{\Delta L}{L_o} \right)^{-3} \qquad (1)$$

where L_o is the initial length and $\Delta L = L_o - L$, where L is the instantaneous sample length. The final density was also measured by the Archimedes method in deionized water. In a separate set of experiments, sintering was terminated after the pre-coarsening step and, following this step, at several temperatures between 800 and 1450 °C (i.e., 1260, 1300, 1350 and 1400 °C). After measurement of the density by the Archimedes method, these samples were used in the microstructural characterization experiments described below.

(3) Microstructural Characterization

A variety of techniques was used to characterize the microstructure of the green compacts and of the sintered samples. The microstructure of fracture surfaces, polished surfaces and polished and thermally etched surfaces was observed by SEM (ISI-DS 130, International Scientific Instruments Inc., Pleasanton, CA), the pore parameters (porosity, average pore size and pore size distribution) were measured by mercury porosimetry (Autopore 9220, Micromeritics Instrument Corp., Norcross, GA) and the specific surface area was determined by nitrogen adsorption by the BET method (Digisorb 2600, Micromeritics Instrument Corp., Norcross, GA) as outlined earlier for the powder. In addition, the amount of closed and open porosity was determined by the Archimedes method in deionized water.

Mercury porosimetry, nitrogen adsorption and SEM of fracture surfaces were the techniques used to characterize the green compacts, the compacts heated conventionally to 800 °C and the compacts subjected to the pre-coarsening step (50 h at 800 °C). For the compacts sintered above 800 °C, the characterization techniques consisted of SEM of polished surfaces and of polished and thermally etched surfaces, mercury porosimetry and water immersion.

In the preparation of polished surfaces for SEM, compacts with low density (~0.65-0.85) were impregnated with epoxy resin prior to polishing. Compacts with higher density were mounted in epoxy resin. Grinding was performed with successively finer diamond wheels and final polishing was accomplished with diamond pastes down to 0.25 μm. After polishing, the

dense samples were removed from the epoxy resin and etched thermally in air for 1 h at 1280 °C. Surfaces of the samples were coated with Au/Pd before observation in the SEM. Grain size was measured from SEM micrographs by the lineal intercept technique [27,28], using more than 500 grains for each sample.

In the mercury porosimetry experiments, the pore diameter was determined from the pressure of intrusion by using the Washburn equation and assuming values of 130° for the contact angle and 485 dyn/cm^2 for the surface tension of mercury [29]. The pore size distributions follow from the derivative of the volume intruded with respect to the pore diameter.

For the determination of the amount of open and closed porosity, the samples were immersed in deionized water (previously boiled to remove air bubbles) and the volume of liquid displaced (the upthrust) was measured by the Archimedes method. After extracting the sample from the water and rapidly removing any adsorbed water on the surface, the volume of liquid intruded (the volume of the open porosity) was determined by weighing the sample. Finally, the difference between the theoretical volume (mass divided by the theoretical density) and the upthrust was taken as the volume of the closed porosity.

III. Results

The experiments provided data for the densification and microstructural evolution of Al_2O_3 powder compacts sintered by the two-step technique and similar compacts sintered conventionally (without the initial pre-coarsening step). The results are described in the following sections.

(1) Microstructural Evolution during the Pre-coarsening Step

During the pre-coarsening step (50 h at 800 °C), no measurable shrinkage was detected in the dilatometer. However, SEM, nitrogen adsorption and mercury porosimetry revealed that significant matter transport had occurred. Figure 1 shows scanning electron micrographs of the

fracture surfaces of a powder compact heated to 800 °C and a compact pre-coarsened for 50 h at 800 °C. Considerable matter transport has occurred in the compact subjected to the pre-coarsening treatment. The particles show more rounding of the edges and corners and the finest have disappeared. There is a small increase in the average particle size of the pre-coarsened compact but the magnitude of the increase is difficult to measure accurately from micrographs.

The nitrogen adsorption experiments showed that the pre-coarsening step resulted in a decrease in the specific surface area from 10.9 to 7.8 m^2/g . As outlined earlier, it has been suggested that these microstructural changes occur by an Ostwald ripening process. Since vapor transport is expected to be negligible in Al_2O_3 at 800 °C, matter transport appears to be fully dominated by surface diffusion [30].

The pore size distribution data (Fig. 2) show that the pre-coarsening step also produced significant changes in the pore parameters. The finest pores have been eliminated and, compared to the conventionally heated compact, the median pore size has shifted to a larger value (from 0.044 to 0.053 μm). Furthermore, the bimodal distribution in pore sizes (measured for the conventionally heated compact) has evolved into a distribution curve with a single peak. The elimination of the smallest pores and the shift in the pore size distribution curve to larger pore sizes are consistent with an Ostwald ripening mechanism. It would be expected that the smallest pores would be eliminated with the disappearance of the finest particles, leading to the creation, on average, of larger intrusion channels in mercury porosimetry. If the tails of the pore size distribution curves at the smallest and largest pore sizes (representing only a very small fraction of the porosity) are ignored, then it is clear that pore size distribution has become more uniform as a result of the pre-coarsening step. These results support a microstructural path for the system in which an initially non-scaling distribution evolves towards a quasi-steady state (scaling) distribution.

To summarize at this stage, the pre-coarsening step for 50 h at 800 °C has resulted in an improvement in the microstructural homogeneity of Al_2O_3 powder compacts. The data indicate

that the average grain size has increased slightly and the specific surface area has decreased. The median pore size has increased, and, for almost all of the porosity, the normalized distribution in pore sizes has become significantly narrower. The next section describes how these microstructural changes influence the subsequent sintering.

(2) Effect of Pre-coarsening on Subsequent Sintering

Figure 3 shows the results for the relative density as a function of temperature during subsequent sintering at 4 °C/min between 800 and 1450 °C for the compacts pre-coarsened for 50 h at 800 °C and for the conventionally sintered compacts. The pre-coarsening step causes a delay in the onset of measurable densification, while the density initially remains lower than that for the conventionally sintered compact. However, at higher temperatures, the densification rate increases more rapidly compared to that for the conventionally sintered compact (Fig. 4) and above ~1350 °C, the pre-coarsened compact has, in fact, a measurably higher density. The delay in the onset of densification for the pre-coarsened compact is likely to be caused by the elimination of the finest particles (and the smallest pores associated with them) during the pre-coarsening step. Local densification associated with the finest particles in the conventionally sintered compact will be significantly reduced in the pre-coarsened compact. Later in the sintering process, the pre-coarsening provides a benefit for densification in that the density (at a given temperature) is slightly higher than that for the conventionally sintered compact.

The variation of open and closed porosity during subsequent sintering is shown in Fig. 5 for the pre-coarsened compact and for the conventionally sintered compact. At the equivalent density, the amount of open porosity is higher and the amount of closed porosity is lower in the pre-coarsened compact. The data therefore show clearly that the pinch-off of the open pores is delayed to higher densities in the pre-coarsened compact.

Scanning electron micrographs of the polished and thermally etched surfaces of compacts sintered to 1200 °C with and without the pre-coarsening treatment are shown in Fig. 6. The

relative densities of the compacts are approximately the same (~0.75). However, local regions of high density have already started to appear in the conventionally sintered sample. Corresponding micrographs for compacts sintered to 1350 °C are shown in Fig. 7. The regions of high density have increased in the conventionally sintered sample whereas the porosity is distributed more uniformly in the pre-coarsened sample. Figure 8 shows scanning electron micrographs of the polished and thermally etched surfaces of the conventionally sintered compact and of the pre-coarsened compact after sintering to 1450 °C. The relative densities of both samples are greater than 0.99. However, there is considerable refinement of the grain size in the pre-coarsened sample. The pre-coarsened sample has a smaller average size and a significantly smaller standard deviation in the average size (1.3 ± 0.1 μm) when compared with the conventionally sintered sample (1.5 ± 0.2 μm). The final density of the pre-coarsened compact is slightly higher than that for the conventionally sintered compact and, as outlined below, the refinement of the final grain size is even more pronounced if the results were to be considered at an equivalent density.

Figure 9 shows the grain size versus density trajectories for the conventionally sintered compact and for the pre-coarsened compact during constant heating rate sintering to several temperatures between 800 and 1450 °C. For relative densities below ~0.95, corresponding to sintering temperatures below ~1350 °C, the effect of the pre-coarsening step is not obvious. However, at higher densities, a significantly steeper trajectory is found for the conventionally sintered compact. The larger average grain size in the conventionally sintered compact results from the contribution of a higher fraction of large grains in the microstructure. At a given relative density, a larger number of highly dense regions is present in the conventionally sintered compact and these regions are better able to support grain growth.

IV. Discussion

Figures 6 to 8 show that the spatial scale over which density variations occur is considerably larger for the conventionally sintered sample and that the scale increases during sintering. If the

scale of the density fluctuations is taken as a measure of the microstructural homogeneity, then it is clear that the microstructure of the pre-coarsened compact evolves in a more homogeneous manner. The more homogeneous evolution of the microstructure is associated with a refinement in the grain size of the final compact (Figs. 8 and 9). In order to understand the microstructural evolution in two-step sintering, the mechanisms that lead to the improvement in the microstructural homogeneity coupled with the refinement in the grain size need to be examined.

(i) Mechanisms for Improvement in Microstructural Homogeneity

As discussed earlier, it has been suggested that a combination of a more uniform microstructure and a stronger compact produced by the pre-coarsening step is responsible for the more homogeneous evolution of the microstructure in subsequent sintering. The results of the present work provides strong support for this proposal. The elimination of the very fine particles as a result of the pre-coarsening treatment (Fig. 1) is expected to reduce the extent of differential densification and the formation of locally dense regions in the early stages of subsequent sintering, thereby reducing the scale of density fluctuations. The enhancement in neck formation for the compact subjected to the pre-coarsening treatment (Fig. 1) is an indication of an improvement in strength. Furthermore, as reported elsewhere [26], compacts were formed, by slip casting, from the same Al_2O_3 powder used in the present experiments and their flexural strength was measured at room temperature by four-point bending. The pre-coarsening treatment produced an enhancement in the strength of ~50 times that for the compact without the pre-coarsening treatment.

The pore characteristics of the pre-coarsened compact can also have a significant effect on the microstructural evolution during sintering. In the literature, many studies have reported on the effect of pore size distribution on densification during conventional sintering [4,19,31,32]. It is generally found that under identical sintering conditions, green compacts with a narrow pore size distribution reach a higher end-point density and have a more homogeneous microstructure

when compared with similar compacts with a broad pore size distribution. These effects have normally been accounted for in terms of an increase in the distance for matter transport into pores that are more widely spaced and the unfavorable thermodynamic requirement for shrinkage of some (large) pores [16,33]. As outlined later, the decay (or pinch-off) of the continuous pore channels during subsequent sintering can also play an important role in the evolution of the microstructure.

(2) Mechanism for Grain Size Refinement

Pores exert a drag on the grain boundaries and, compared to the pore-free material, can inhibit grain growth [5,34,35]. Large, continuous pores in the initial and intermediate stages of sintering provide a greater drag and, hence, can inhibit grain growth more effectively compared to small, isolated pores in the final stage of sintering. This can give rise to a transition in grain growth behavior, as observed for Al_2O_3 powder compacts formed by a colloidal route [36]. The effects are also seen from plots of the grain size versus density during sintering where the trajectory normally becomes significantly steeper above a relative density of ~0.90. The delay in the pinch-off of the continuous pores has been suggested as a mechanism to explain the grain size refinement during subsequent sintering of the pre-coarsened compacts [9]. The results for the open and closed porosity (Fig. 5) provide clear experimental support for this proposal. The semi-quantitative model of Chu et al [9] for the evolution of the interpore spacing during the sintering of ZnO, as outlined earlier, also provide support for the suggested mechanism. However, the process by which the pore channel pinch-off is delayed in the pre-coarsened compact is unclear. In the next section, pore closure is considered.

(3) Analysis of Pore Closure During Sintering

Physically, the closure of continuous pores during sintering may be expected to influence the microstructural homogeneity (taken as the scale of density fluctuations) and the grain size

characteristics in the following way. For a distribution of pore sizes, early closure of some pores, leading to pinch-off of the pore channels and the creation of smaller, isolated pores can lead to locally dense regions (i.e., to an increase in the scale of density fluctuations) which are better able to support grain growth. Faster grain growth in the dense regions coupled with slower growth in the regions with continuous pores is expected to lead to a wider spread in grain sizes and a larger average size at an equivalent density when compared to a similar system with a more uniform distribution of pore sizes.

The complex nature of the interconnected pore channel network in real powder compacts makes the modeling of pore channel decay difficult [37,38]. The instability of simple shapes has been analyzed and it would be interesting to explore whether those results provide an insight into the decay of the continuous pore channels in real systems. Since the work of Rayleigh [39] who analyzed jets of fluids, the instability of cylindrical shapes under the influence of capillarity or surface tension effects has been well recognized. Much later, Nicholls and Mullins [40] analyzed the instability of an infinite cylinder in which matter transport occurred by surface diffusion and volume diffusion. In other publications, Nicholls and Mullins [41] treated the spheroidization of semi-infinite rods by the mechanism of surface diffusion while Nicholls [42] analyzed the instability of finite cylinders with hemispherical ends.

Recently, Stüwe and Kolednik [43] developed a simple dynamic model to describe the disintegration, by surface diffusion, of cylindrical pores into spheres during the annealing of potassium-doped tungsten. They assumed a model (Fig. 10) consisting of a cylindrical pore of mean radius s weakly disturbed by a sinusoidal fluctuation of amplitude A and wavelength l. The variation in the radius of the cylinder with distance x in the axial direction is described by:

$$r = s + A \sin\frac{2\pi}{l}x \qquad (2)$$

From an analysis of the transport of tungsten atoms from the "bulge" of the cylinder to the

adjacent "necks", Stüwe and Kolednik derived the following equation for the growth rate of the amplitude of fluctuation:

$$\frac{dA}{dt} = \frac{D_s \gamma}{2 \nu \zeta kT} \left(\frac{\delta}{R} \right)^4 ZA \qquad (3)$$

where D_s is the surface diffusion coefficient, γ is the specific surface energy of the solid/vapor interface, ν is the mean diffusion path (expressed as a fraction of the wavelength l), ζ is a geometrical parameter, k is the Boltzmann constant, T is the temperature, δ is the atomic diameter, R is the radius of the unperturbed cylinder, and Z is a parameter defined by :

$$Z = \frac{z^2 - 4\pi^2}{z^4} \qquad (4)$$

where z = l/R.

Equations (3) and (4) show that the growth rate of the amplitude of the fluctuation is positive for $z > 2\pi$ with a maximum growth rate at $z = 2\sqrt{2}\,\pi \approx 8.9$. Furthermore, they show that the magnitude and direction of the growth rate depend only on the amplitude and wavelength (relative to the cylinder radius) of the fluctuation. Two cases can be distinguished. When the volume of the cylinder remains constant (corresponding to the practical case of no densification), R and Z are constant and Eq. (3) can be integrated to determine the variation of A with time [43]. For the case when the volume of the cylinder (pore) decreases with time (i.e., densification occurs), if it is assumed, for the sake of illustration, that the pore volume decreases linearly with time, then:

$$R^2 = R_o^2 - Kt \qquad (5)$$

where R_o is the initial radius of the cylinder and K is a constant. For a sinusoidal fluctuation, R is related to s by the equation[43]:

$$s = R\left(1 - \frac{A^2}{2R^2}\right)^{1/2} \qquad (6)$$

According to Bennison and Harmer [44], the surface diffusivity ($\delta_s D_s$) of undoped Al_2O_3 is $\approx 10^{-21}$ m^3s^{-1} at 1400 °C. Taking $\delta_s \approx 0.2$ nm, then $D_s \approx 10^{-12}$ m^2s^{-1}. Assuming this value for D_s, $\gamma \approx 1$ J/m^2, $\nu \approx \zeta \approx 1/3$, $\delta \approx 0.2$ nm, and that the condition A(t) = R provides an estimate of the time, τ_c, for closure of the cylinder, Eq. (3) was integrated numerically to determine τ_c as a function of A/s for two values of the rate constant K for pore closure (densification). The results (Fig. 11) indicate that τ_c depends strongly on the ratio A/s (as discussed earlier) and on K (i.e., the densification rate).

In considering the experimental data, it should be realized that the mercury porosimetry data provide an estimate of the size of the intrusion channels into the pores. The data in Fig. 2 can therefore be taken to indicate that the pre-coarsening treatment, in which the smallest particles disappear by an Ostwald ripening process, leads to the development of a smoother, more uniform pore channel. This can be taken to mean that the amplitude of the fluctuations in the pore diameter is reduced. The time for pinch-off of the pore channels will therefore increase (Fig. 11).

To summarize, the microstructural refinement produced by the two-step sintering technique is illustrated schematically in Fig. 12. Compared to the conventionally sintered compact, the reduction in differential densification in the early stages of sintering leads to a reduction in the spatial scale of the density fluctuations. The smoother pore channels lead to a delay in the pore channel pinch-off to higher densities, thereby producing a smaller average grain size with a more uniform distribution of grain sizes.

V. Conclusions

The main factors responsible for the microstructural refinement of Al_2O_3 powder compacts

during sintering by a two-step technique were identified. The initial pre-coarsening step produced enhanced neck formation between the particles (thereby leading to a stronger compact) the elimination of the finest particles (presumably by an Ostwald ripening process), a larger median pore size and, importantly, a narrower distribution in pore sizes. The microstructural path is one in which the system evolves from an intially wide distribution to a (normalized) narrower quasi-steady state one. In subsequent sintering, the stronger compact is better able to resist differential densification while the elimination of the finest particles reduces local densification. These two factors lead to a reduction in the spatial scale of density fluctuations, i.e., to a more homogeneous microstructure. If the larger median pore size and the narrower distribution in pore sizes (determined from mercury porosimetry) are taken to represent the formation of smoother pore channels, theoretical models predict an increase in the time for pinch-off of the continuous pore channels. The delay in pore channel pinch-off is supported by data for the open and closed porosity during sintering. The pores therefore remain open to higher densities, thereby inhibiting grain growth more effectively. In this way, a more homogeneous sintered microstructure coupled with a smaller average grain size and a narrower distribution in grain sizes is produced.

References

1. R. J. Brook, "Fabrication Principles for the Production of Ceramics with Superior Mechanical Properties," *Proc. Br. Ceram. Soc.*, **32**, 7-24 (1982).

2. E. A. Barringer and H. K. Bowen, "Formation, Packing, and Sintering of Monodispersed TiO_2 Powders," *J. Am. Ceram. Soc.*, **65** [10] C-199 - C-201 (1982).

3. I. A. Aksay, "Microstructure Control through Colloidal Consolidation"; pp. 94-104 in *Advances in Ceramics, Vol. 9: Forming of Ceramics*. Edited by J. A. Mangels and G. L. Messing. The American Ceramic Society, Columbus, OH, 1984.

4. T.-S. Yeh and M. D. Sacks, "Low-Temperature Sintering of Aluminum Oxide," *J. Am. Ceram. Soc.*, **71** [10] 841-44 (1988).

5. R. J. Brook, "Controlled Grain Growth"; pp. 331-364 in *Treatise on Materials Science and Technology, Vol. 9: Ceramic Fabrication Processes*. Edited by F. F. W. Wang. Academic Press, New York, 1976.

6. M. P. Harmer, "Use of Solid Solution Additives in Ceramic Processing"; pp. 679-96 in *Advances in Ceramics, Vol. 10: Structure of MgO and Al_2O_3 Ceramics*. Edited by W. D. Kingery. The American Ceramic Society, Columbus, OH, 1984

7. M. N. Rahaman, *Ceramic Processing and Sintering*, Marcel Dekker, New York, 1995.

8. R. M. German, *Liquid Phase Sintering*, Plenum Press, New York, 1985.

9. M.-Y. Chu, L. C. De Jonghe, M. F. K. Lin, and F. J. T. Lin, "Precoarsening to Improve Microstructure and Sintering of Powder Compacts," *J. Am. Ceram. Soc.*, **74** [11] 2902-11 (1991).

10. H. Pickup, U. Eisele, E. Gilbart, and R. J. Brook, "Analysis of Coarsening and Densification Kinetics during the Heat Treatment of Nitrogen Ceramics"; pp. 41-51 in *Non-Oxide Technical and Engineering Ceramics*. Edited by S. Hampshire. Elsevier Applied Science, New York, 1985.

11. M. P. Harmer, E. W. Roberts, and R. J. Brook, "Rapid Sintering of Pure and Doped a-Al_2O_3," *Trans. J. Br. Ceram. Soc.*, **78**, 22-25 (1979).

12. H. Mostaghaci and R. J. Brook, "Fast Firing of Barium Titanate," *Trans. Br. Ceram. Soc.*, **82** [5] 167-69 (1983).

13. H. Palmour III and D. R. Johnson, "Phenomenological Model for Rate-Controlled Sintering"; pp. 777-92 in *Sintering and Related Phenomena*. Edited by G. C. Kuczynski, N. A. Hooton, and C. F. Gibbon. Gordon and Breach, New York, 1967.]

14. J. H. Duncan and W. G. Budgen , "Two-Peak Firing of Beta''-Alumina", *Proc. Brit. Ceram. Soc.*, **31,** 221-32 (1981). Special Ceramics 7. Edited by D. Taylor and P. Popper . The British Ceramic Society, Stoke-on-Trent, 1981.

15. W. H. Rhodes, "Agglomerate and Particle Size Effects on Sintering Yttria-Stabilized Zirconia," *J. Am. Ceram. Soc.*, **64** [1] 19-22 (1981).

16. F. F. Lange, "Sinterability of Agglomerated Powders," *J. Am. Ceram. Soc.*, **67** [2] 83-89 (1984).

17. F. W. Dynys and J. W. Halloran, "Influence of Aggregates on Sintering," *J. Am. Ceram. Soc.*, **67** [9] 596-601 (1984).

18. F. F. Lange and B. I. Davis, "Sinterability of ZrO_2 and Al_2O_3 Powders: The Role of Coordination Number Distribution"; pp. 699-713 in *Advances in Ceramics, Vol. 10: Science and Technology of Zirconia II.* Edited by N. Claussen, M. Ruhle, and A. H. Heuer. The American Ceramic Society, Columbus, OH, 1984.

19. A. Roosen and H. Hausner, "Sintering Kinetics of ZrO_2 Powders"; pp. 714-26 in *Advances in Ceramics, Vol. 10: Science and Technology of Zirconia II.* Edited by N. Claussen, M. Ruhle, and A. H. Heuer. The American Ceramic Society, Columbus, OH, 1984.

20. A. Roosen and H. K. Bowen, "Influence of Various Consolidation Techniques on the Green Microstructure and Sintering Behavior of Alumina Powders," *J. Am. Ceram. Soc.*, **71** [11] 970-77 (1988).

21. A. G. Evans, "Considerations of Inhomogeneity Effects in Sintering," *J. Am. Ceram. Soc.*, **65** [10] 497-501 (1982).

22. M. Weiser and L. C. De Jonghe, "Rearrangement During Sintering in Two-Dimensional Arrays," *J. Am. Ceram. Soc.*, **69** [11] 822-26 (1986).

23. M. Lin, M. N. Rahaman, and L. C. De Jonghe, "Creep-Sintering and Microstructure Development of Heterogeneous MgO Compacts," *J. Am. Ceram. Soc.*, **70** [5] 360-66 (1987).

24. M. K.-F. Lin, "Sintering of Heterogeneous MgO Compacts"; Ph.D. Thesis, University of California at Berkeley, April 1988.

25. M.-Y. Chu, "Sintering Stress and Microstructure in Ceramic Powder Compacts"; Ph.D. Thesis, University of California at Berkeley, August 1990.

26. F. J. T. Lin, "Microstructure Improvement of Alumina by a Two-Step Sintering Technique"; Ph.D. Thesis, University of California at Berkeley, May 1992.

27. M. I. Mendelson, "Average Grain Size in Polycrystalline Ceramics," *J. Am. Ceram. Soc.*, **52** [8] 443-46 (1969).

28. J. C. Wurst and J. A. Nelson, "Lineal Intercept Technique for Measuring Grain Size in Two-Phase Polycrystalline Ceramics," *J. Am. Ceram. Soc.*, **55** [2] 109 (1972).

29. T. Allen, *Particle Size Measurement*, 3rd ed., Chapman and Hall, New York, 1981.

30. S. Prochazka and R. L. Coble, "Surface Diffusion in the Initial Sintering of Alumina: III," *Phys. Sintering*, **2** [2] 15-33 (1970).

31. T. J. Carbone and J. S. Reed, "Dependence of Sintering Response with a Constant Rate of Heating on Processing-Related Pore Distribution," *Am. Ceram. Soc. Bull.*, **57** [8] 748-50 (1978).

32. T.-S. Yeh and M. D. Sacks, "Effect of Green Microstructure on Sintering of Alumina"; pp. 309-31 in *Ceramic Transactions, Vol. 7: Sintering of Advanced Ceramics*. Edited by C. A. Handwerker, J. E. Blendell, and W. Kaysser. The American Ceramic Society, Westerville, OH, 1990.

33. W. D. Kingery and B. Francois, "Sintering of Crystalline Oxides, I. Interactions between Grain Boundaries and Pores"; pp. 471-98 in *Sintering and Related Phenomena*. Edited by G. C. Kuczynski, N. A. Hooton, and C. F. Gibbon. Gordon and Breach, New York, 1967.

34. R. J. Brook, "Pore-Grain Boundary Interactions and Grain Growth," *J. Am. Ceram. Soc.*, **52** [1] 56-57 (1969).

35. F. M. A. Carpay, "The Effect of Pore Drag on Ceramic Microstructure"; pp. 261-75 in *Ceramic Microstructure '76*. Edited by R. M. Fulrath and J. A. Pask. Westview Press, Boulder, CO, 1977.

36. C. P. Cameron and R. Raj, "Grain Growth Transition during Sintering of Colloidally Prepared Alumina Powder Compacts," *J. Am. Ceram. Soc.*, **71** [12] 1031-35 (1988).

37. R. T. DeHoff, "A Cell Model for Microstructurasl Evolution during Sintering"; pp. 23-34 in *Materials Science Research, Vol. 16*. Edited by G. C. Kuczynski, A. E. Miller, and G. A. Sargent. Plenum Press, New York, 1984.

38. F. N. Rhines and R. T. DeHoff, "Channel Network Decay in Sintering"; pp. 49-61 in *Materials Science Research, Vol. 16*. Edited by G. C. Kuczynski, A. E. Miller, and G. A. Sargent. Plenum Press, New York, 1984.

39. Lord Rayleigh, "On the Instability of Jets," *Proc. London Math. Soc.*, **10**, 4-13 (1879).

40. F. A. Nicholls and W. W. Mullins, "Surface- (Interface-) and Volume-Diffusion Contributions to Morphological Changes Driven by Capillarity," *Trans. Met. Soc. AIME*, **233**, 1840-55 (1965).

41. F. A. Nicholls and W. W. Mullins, "Morphological Changes of a Surface of Revolution due to Capillarity-Induced Surface Diffusion," *J. Appl. Phys.*, **36**, 1826-35 (1965).

42. F. A. Nicholls, "On the Spheroidization of Rod-Shaped Particles of Finite Length," *J. Mater. Sci.*, **11**, 1077-82 (1976).

43. H. P. Stüwe and O. Kolednik, "Shape Instability of Thin Cylinders," *Acta metall.*, **36** [7] 1705-08 (1988).

44. S. J. Bennison and M. P. Harmer, "Effect of Magnesia Solute on Surface Diffusion in Sapphire and the Role of Magnesia in the Sintering of Alumina," *J. Am. Ceram. Soc.*, **73** [4] 833-37 (1990).

Figure Captions

Figure 1. SEM of the fracture surfaces of (a) an Al_2O_3 compact after heating at 10 °C/min to 800 °C (denoted "conventional") and (b) a similar compact after a pre-coarsening treatment for 50 h at 800 °C.

Figure 2. Pore size distribution as a function of pore diameter obtained from mercury porosimetry for the compacts described in Fig. 1.

Figure 3. Relative density versus temperature during constant heating rate sintering (4 °C/min) for a compact heated conventionally (i.e., without the pre-coarsening step) and for a compact pre-coarsened for 50 h at 800 °C.

Figure 4. Densification rate versus temperature for the compacts described in Fig. 3.

Figure 5. The amount of open and closed porosity versus relative density during sintering for a conventionally sintered compact and for a pre-coarsened compact (800 °C/50 h).

Figure 6. SEM of the polished and thermally etched surfaces of (a) a conventionally sintered compact (relative density = 0.76) and (b) a pre-coarsened compact (relative density = 0.73) after heating at 4 °C/min to 1200 °C.

Figure 7. SEM of the polished and thermally etched surfaces of (a) a conventionally sintered compact (relative density = 0.93) and (b) a pre-coarsened compact (relative density = 0.93) after heating at 4 °C/min to 1350 °C.

Figure 8. SEM of the polished and thermally etched surfaces of (a) a conventionally sintered compact (relative density = 0.99; grain size = 1.5 ± 0.2 μm) and (b) a pre-coarsened compact (relative density = 0.99; grain size = 1.3 ± 0.1 μm) after heating at 4 °C/min to 1450 °C.

Figure 9. Grain size versus density trajectories for the conventionally sintered compact and the pre-coarsened compact (800 °C/50 h) during constant heating rate sintering to temperatures between 800 and 1450 °C.

Figure 10. Schematic diagram showing the geometrical parameters for a cylindrical pore of average radius s which contains a sinusoidal fluctuation of amplitude A and wavelength l.

Figure 11. Model predictions for the time to pinch-off of a cylindrical pore as a function of A/s (the ratio of the amplitude of the fluctuation to the average radius of the cylinder) for two values of the rate constant K for pore closure (shown in $\mu m^2 s^{-1}$).

Figure 12. Schematic diagram illustrating the microstructural refinement produced by the two-step sintering technique.

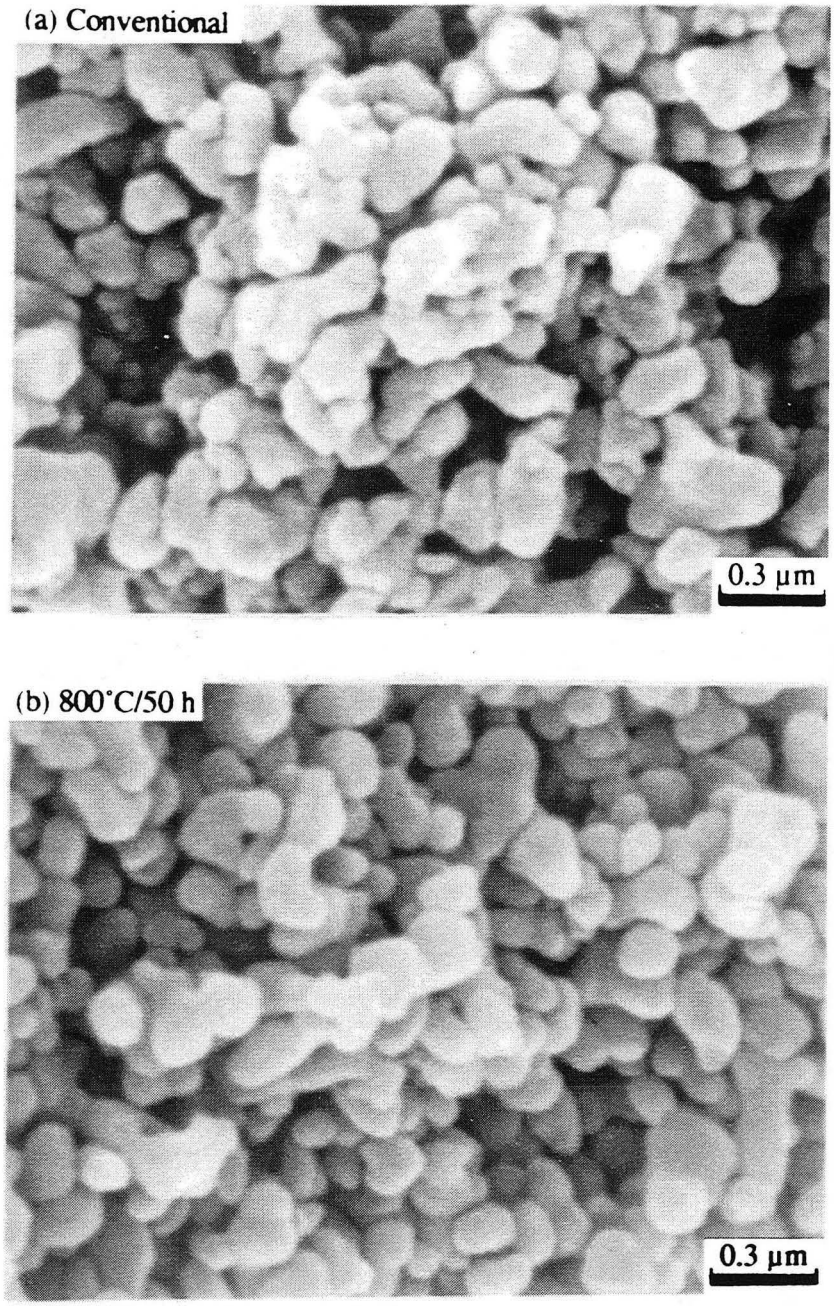

Figure 1

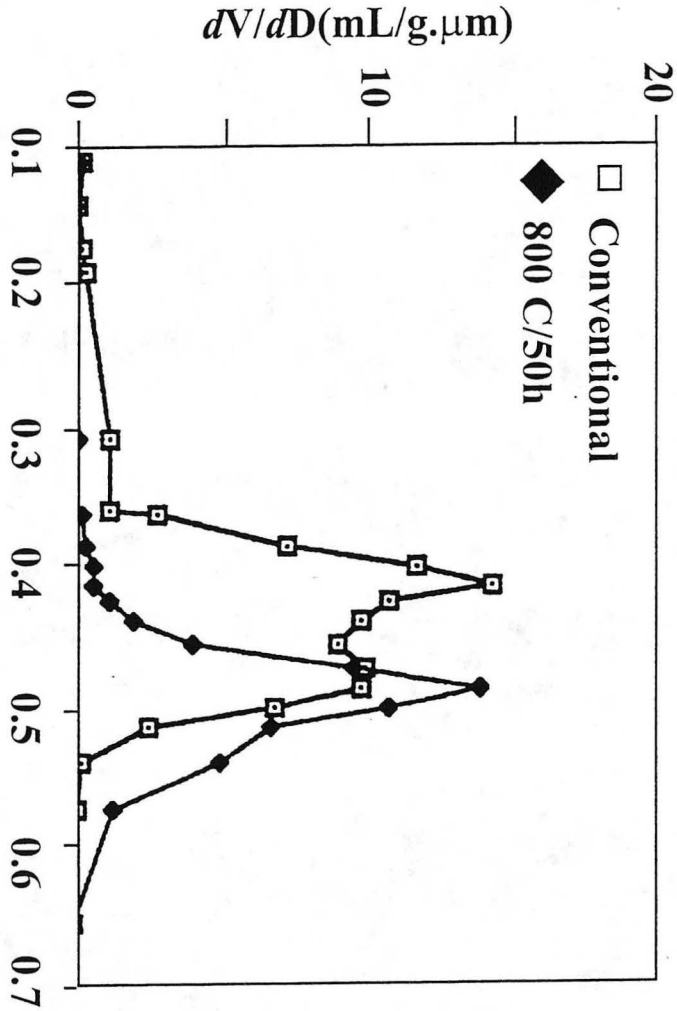

Figure 2

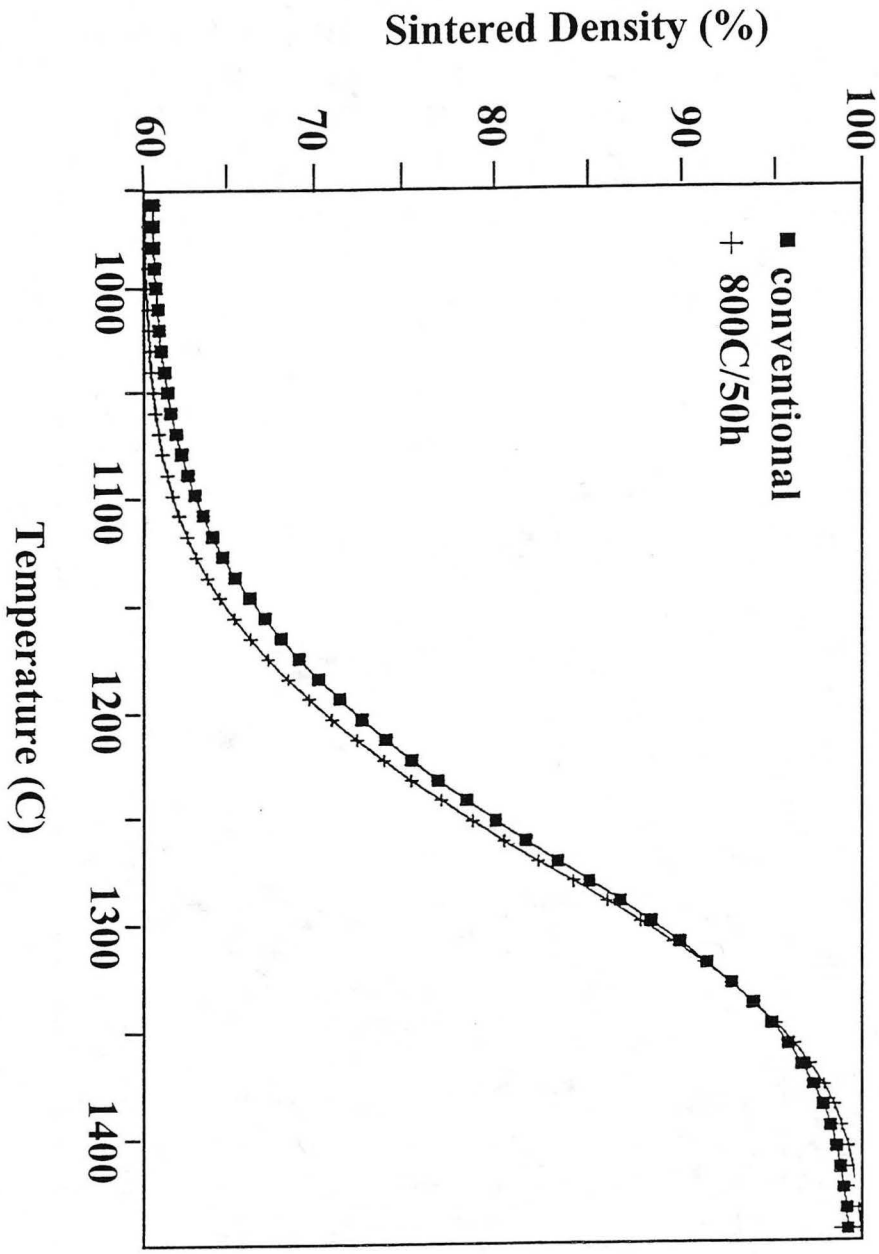
Sintered Density (%)
100
90
80
70
60
■ conventional
+ 800C/50h
1000
1100
1200
1300
1400
Temperature (C)

Figure 3

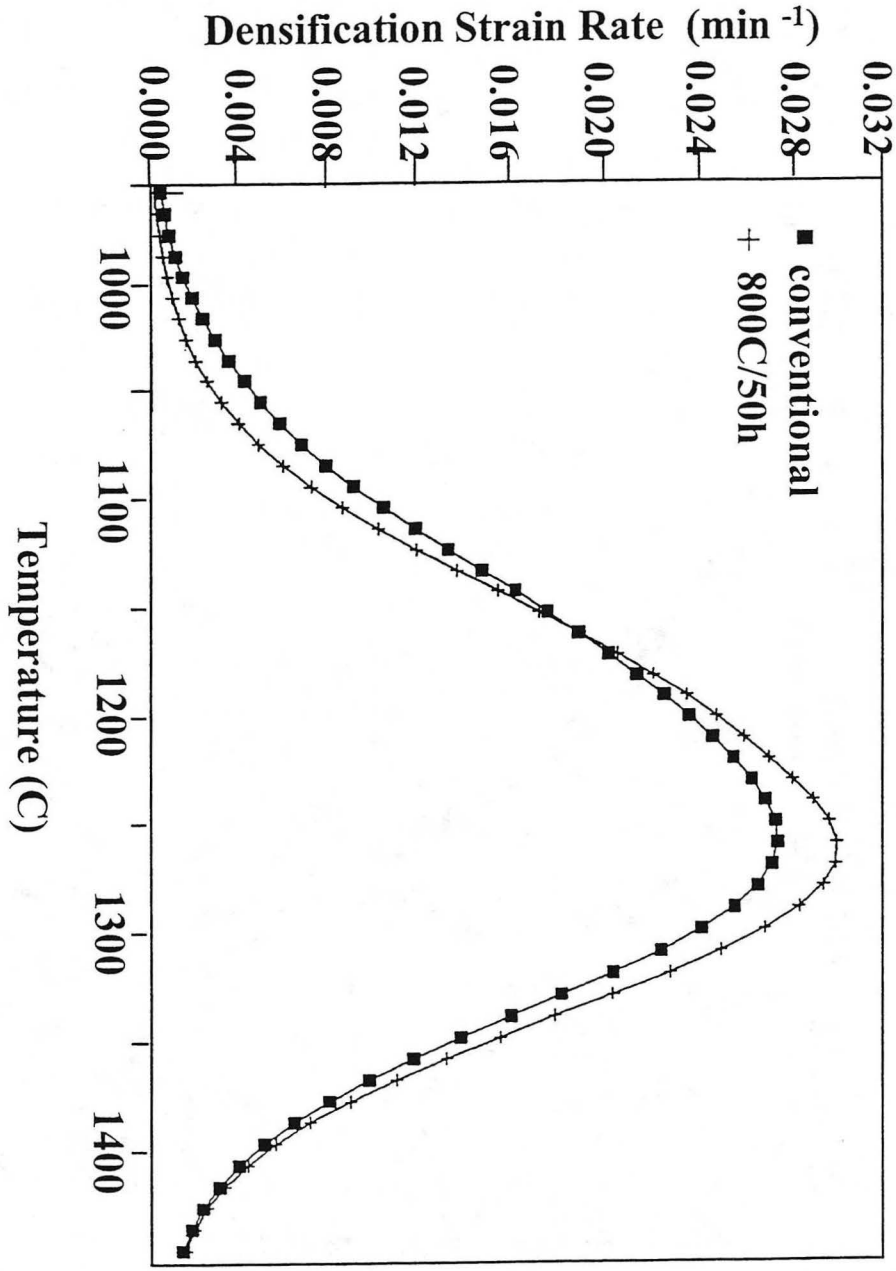
Densification Strain Rate (min -1)
0.032
0.028
0.024
0.020
0.016
0.012
0.008
0.004
0.000
■ conventional
+ 800C/50h
1000
1100
1200
1300
1400
Temperature (C)

Figure 4

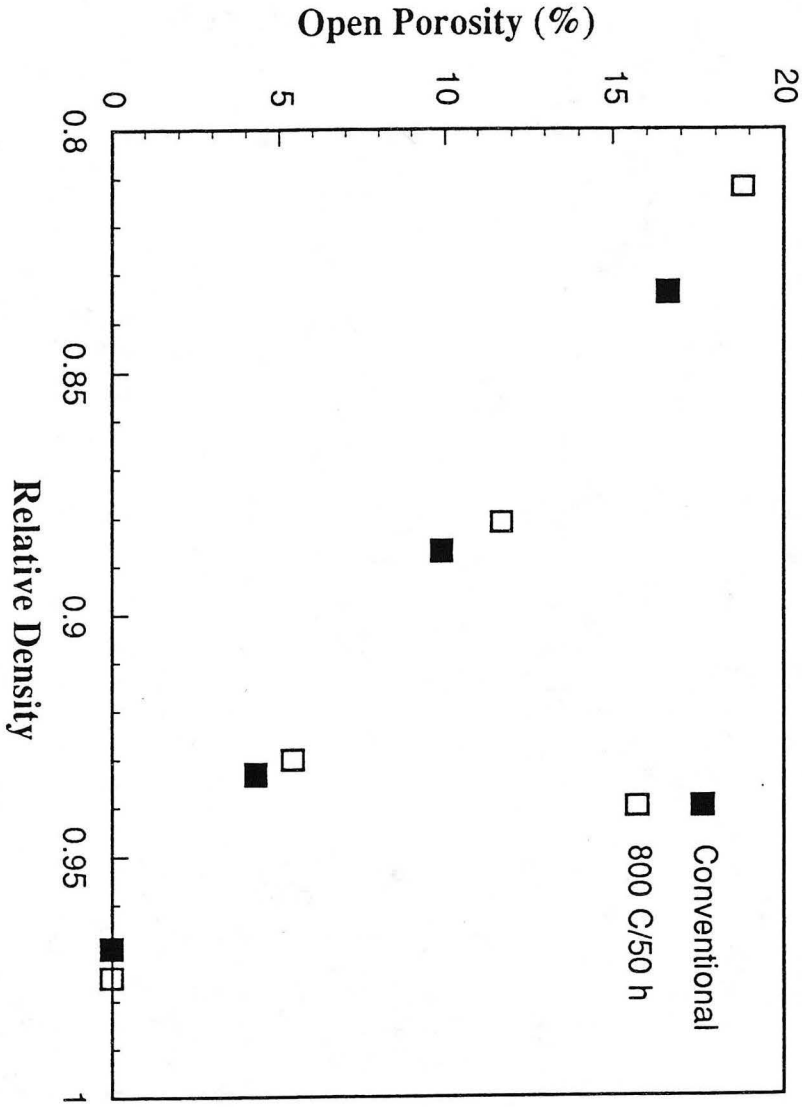
Open Porosity (%)
20
15
10
5
0
0.8
0.85
0.9
0.95
1
Relative Density
Conventional
800 C/50 h

Figure 5(a)

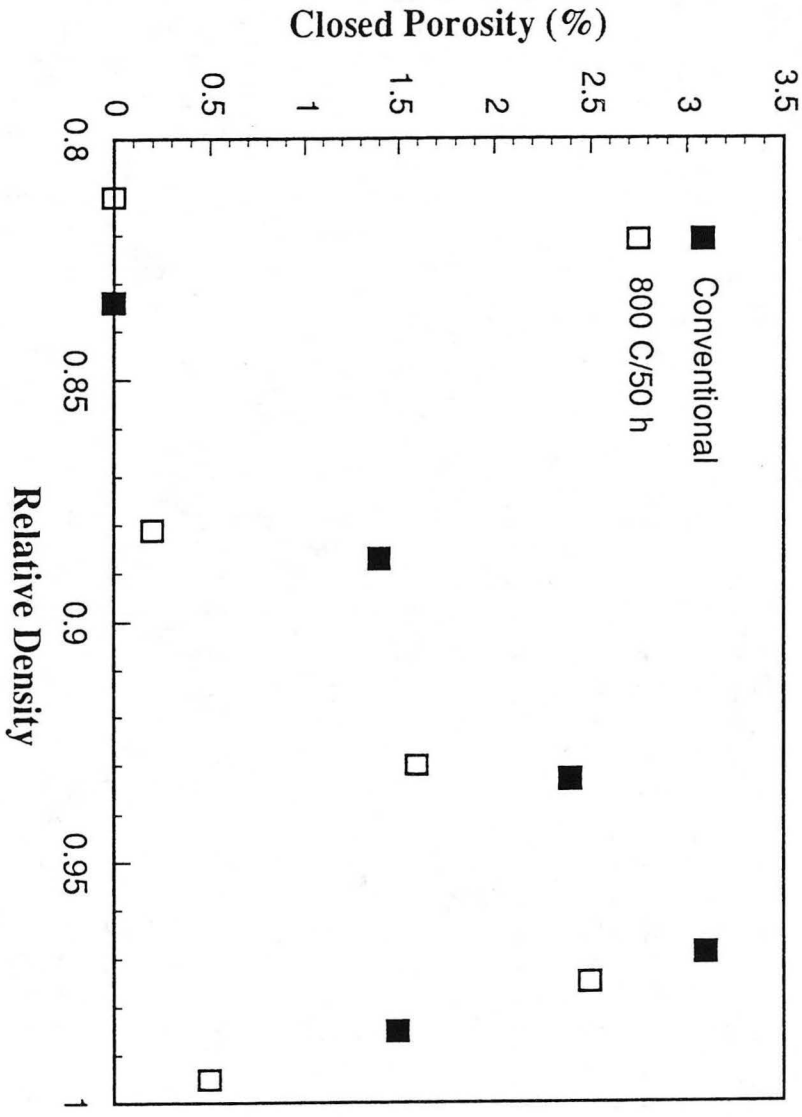
Closed Porosity (%)
3.5
3
2.5
2
1.5
1
0.5
0
Conventional
800 C/50 h
0.8
0.85
0.9
0.95
1
Relative Density

Figure 5(b)

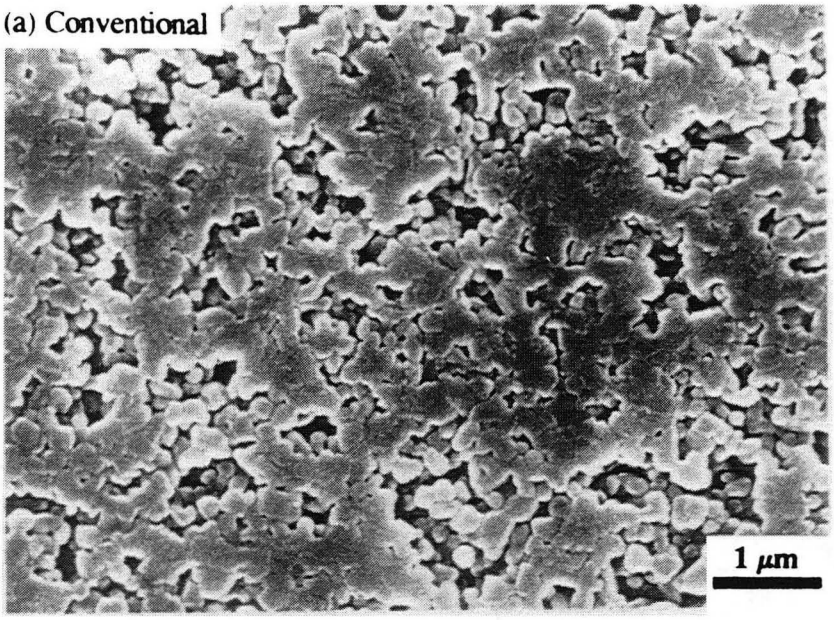

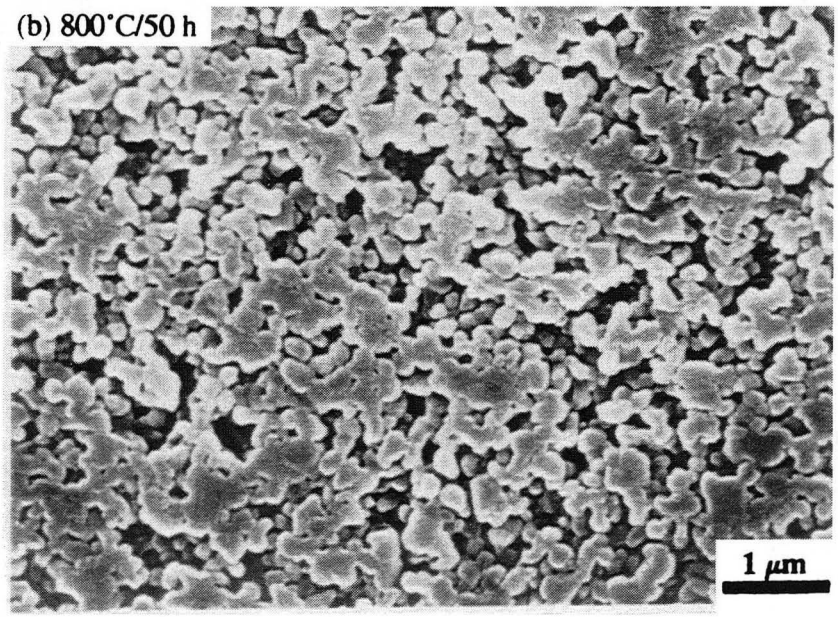

Figure 6

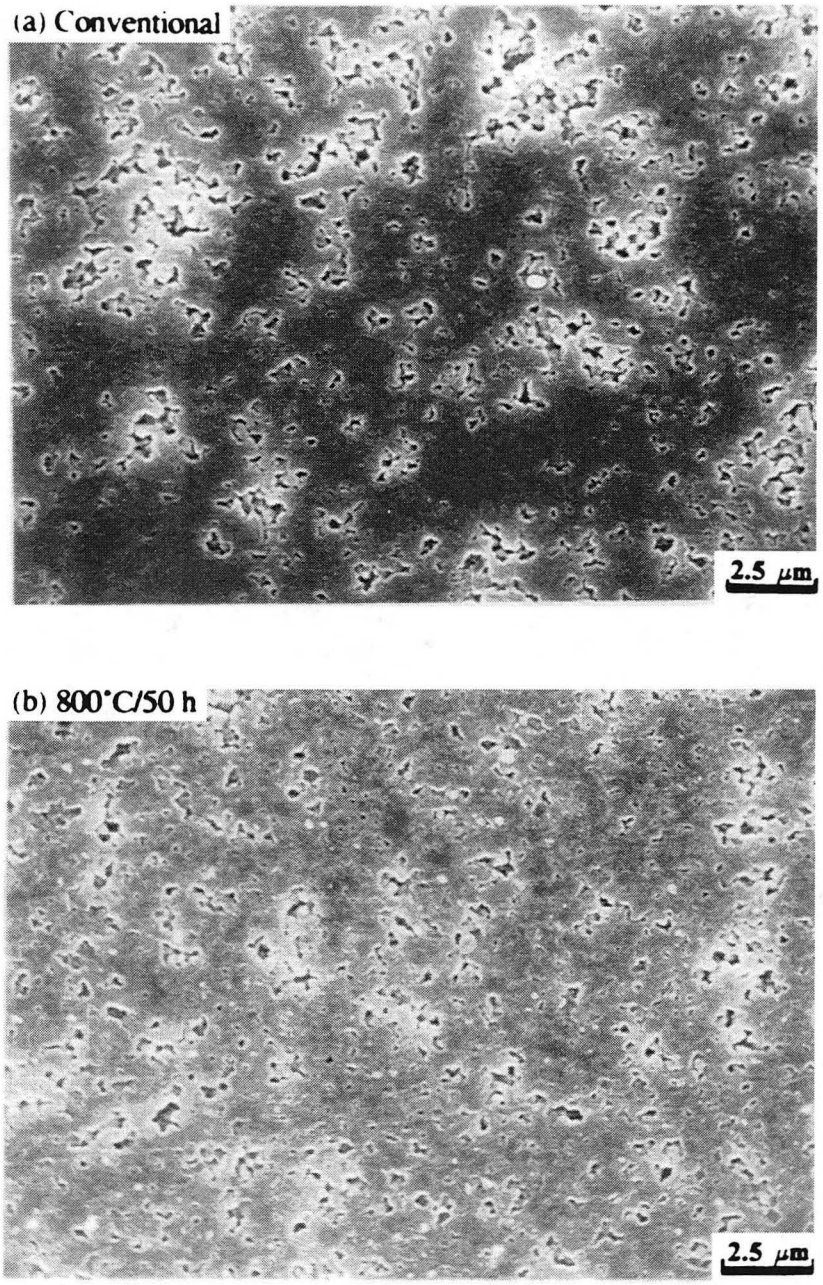

Figure 7

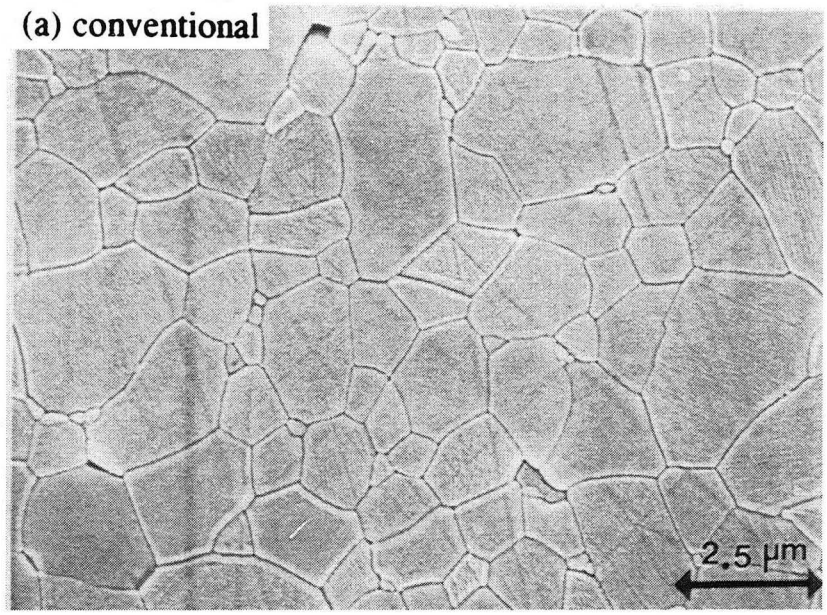

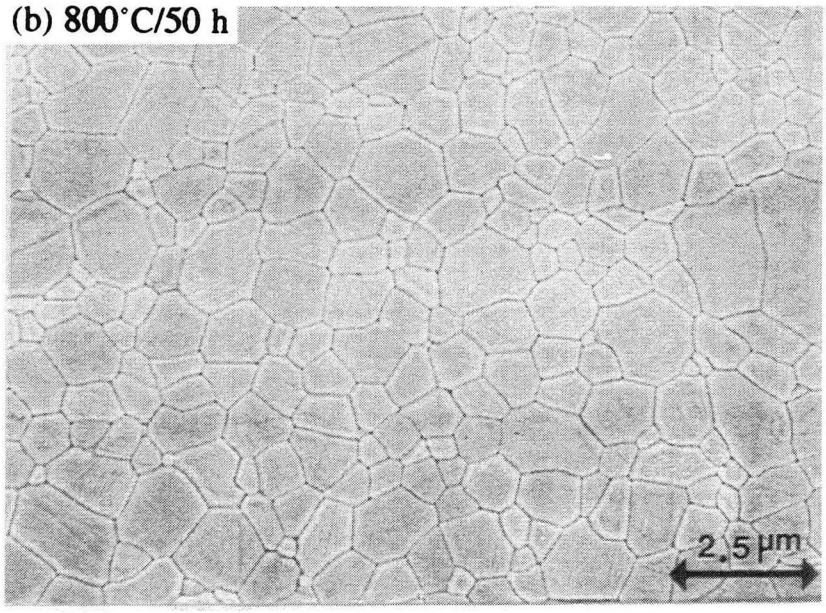

Figure 8

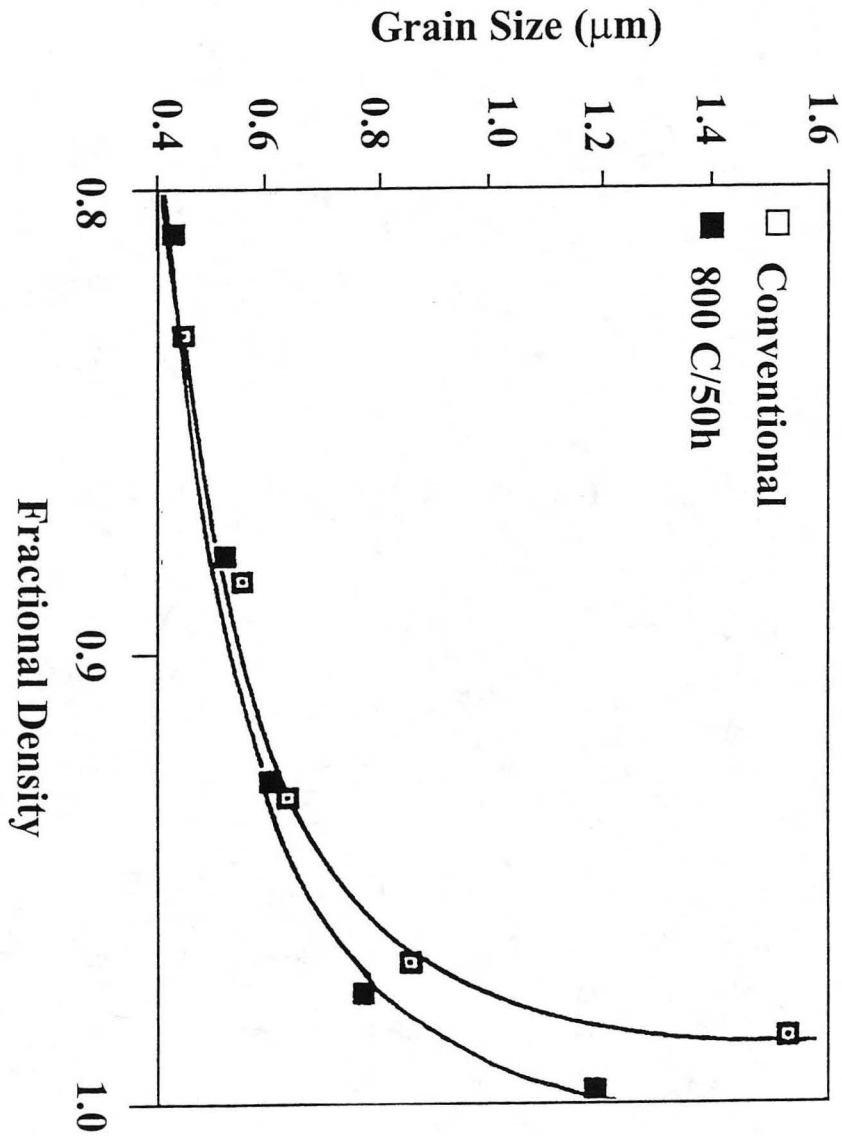
Grain Size (μm)
1.6
1.4
1.2
1.0
0.8
0.6
0.4
Conventional
800 C/50h
0.8
0.9
1.0
Fractional Density

Figure 9

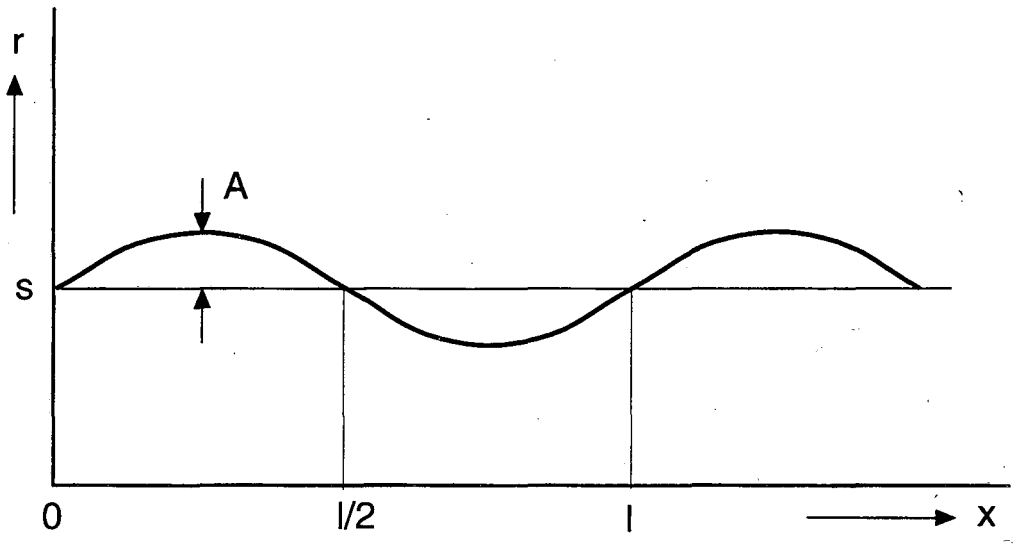

Figure 10

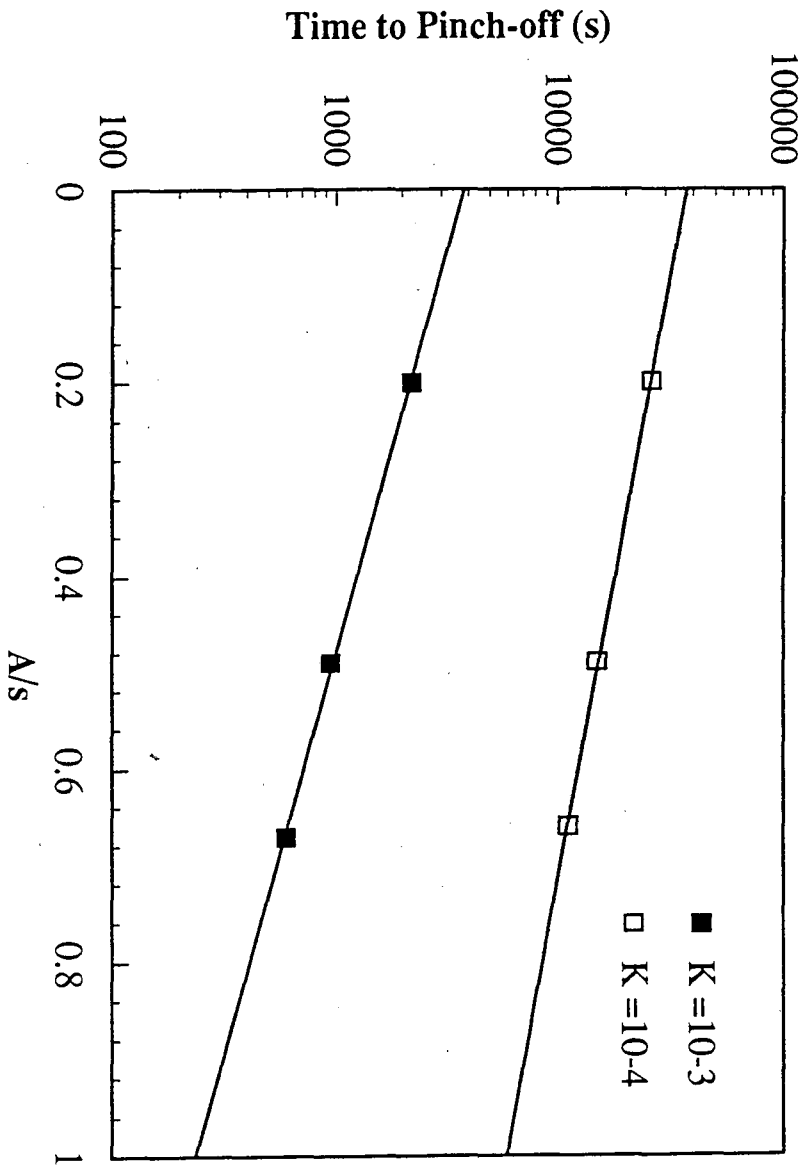
Time to Pinch-off (s)
100000
10000
1000
100
0
0.2
0.4
0.6
0.8
1
A/s
K =10-3
K =10-4

Figure 11

Conventional

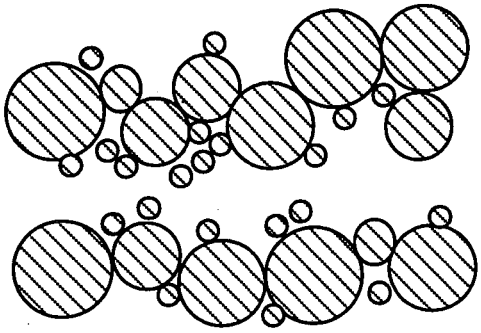

Direct Sintering

Small particles densify faster
Uneven pore size distribution

To later stage
of sintering

Non-uniform grain size
distribution
(Some very large grains)

Residual porosity

Two-Step

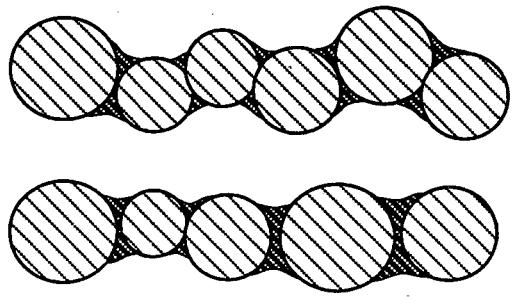

Pore channel becomes
smoother after pre-coarsening

Sintering

Differential densification reduced
in the early stage of sintering

To later stage
of sintering

Delay of pore channel pinch-off
to later stage of sintering

Figure 12

Ernest Orlando Lawrence Berkeley National Laboratory
One Cyclotron Road | Berkeley, California 94720

Prepared for the U.S. Department of Energy under Contract No. DE-AC03-76SF00098